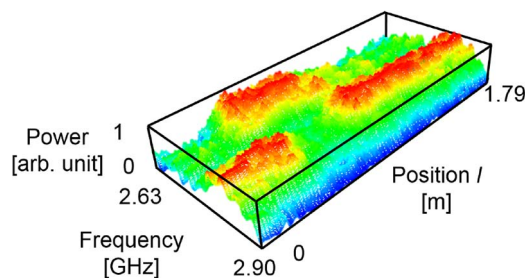


# Simplified Brillouin Optical Correlation-Domain Reflectometry Using Polymer Optical Fiber

Volume 7, Number 1, February 2015

Neisei Hayashi  
Yosuke Mizuno, Member, IEEE  
Kentaro Nakamura, Member, IEEE



DOI: 10.1109/JPHOT.2014.2381650  
1943-0655 © 2014 IEEE

# Simplified Brillouin Optical Correlation-Domain Reflectometry Using Polymer Optical Fiber

Neisei Hayashi, Yosuke Mizuno, *Member, IEEE*, and  
Kentaro Nakamura, *Member, IEEE*

Precision and Intelligence Laboratory, Tokyo Institute of Technology, Yokohama 226-8503, Japan

DOI: 10.1109/JPHOT.2014.2381650

1943-0655 © 2014 IEEE. Translations and content mining are permitted for academic research only.

Personal use is also permitted, but republication/redistribution requires IEEE permission.

See [http://www.ieee.org/publications\\_standards/publications/rights/index.html](http://www.ieee.org/publications_standards/publications/rights/index.html) for more information.

Manuscript received October 14, 2014; revised November 26, 2014; accepted December 3, 2014. Date of publication January 13, 2015; date of current version January 27, 2015. This work was supported in part by Grants-in-Aid for Young Scientists (A) under Grant 25709032 and for Challenging Exploratory Research under Grant 26630180 from the Japan Society for the Promotion of Science (JSPS) and in part by research grants from the Iwatani Naoji Foundation and the SCAT Foundation. The work of N. Hayashi was supported by the Grant-in-Aid for JSPS Fellows under Grant 25007652. Corresponding author: N. Hayashi (e-mail: hayashi@sonic.pi.titech.ac.jp).

**Abstract:** To perform distributed strain and temperature measurement, we have recently developed simplified Brillouin optical correlation-domain reflectometry (S-BOCDR), in which the light that is Fresnel reflected at the ends of the fiber under test (FUT) is used as a reference light. Here, we implement S-BOCDR using a polymer optical fiber (POF) as an FUT, which provides the following advantages over S-BOCDR using a standard silica single-mode fiber (SMF): 1) The beat signal of the Stokes light and the Fresnel-reflected light that is obtained at the interface between the POF and the SMF (the pigtail of an optical circulator) can be stabilized, and 2) the effect of the zeroth correlation peak can be easily and effectively suppressed by exploiting a so-called Brillouin frequency shift-hopping phenomenon. We then experimentally demonstrate a distributed measurement and detect a 0.46-m-long heated POF section.

**Index Terms:** Brillouin scattering, distributed measurement, optical fiber sensors, polymer optical fibers, strain sensing, temperature sensing.

## 1. Introduction

Brillouin scattering in optical fibers has attracted considerable attention [1] and has been applied to a variety of research fields, such as lasing [1], microwave signal processing [2], optical memory [3], phase conjugation [4], and slow light generation [5]. Strain and temperature sensing [6]–[10] is one of the most promising applications because of its ability to measure the strain and temperature distributions along an optical fiber. To date, several distributed sensing techniques have been developed, such as Brillouin optical time-domain analysis and reflectometry (BOTDA/R) [6], [7], [11]–[13], Brillouin optical frequency-domain analysis (BOFDA) [8], [14], [15], and Brillouin optical correlation-domain analysis and reflectometry (BOCDA/R) [9], [10], [16]–[20]. Each technique has its own unique advantages; here, we focus on BOCDR [10], [19], [20], which is the only technique that can simultaneously provide substantial one-end accessibility, high spatial resolution, high sampling rate, and cost efficiency.

Recently, we have developed two schemes of simplified (S-) BOCDR [21], [22], both of which use the light Fresnel-reflected at one end of the fiber under test (FUT) as reference light and do

not include an additional reference path used in the standard configuration. The first configuration (S-BOCDR-1) [21] uses the light Fresnel-reflected at the distal end of the FUT (i.e., open end), whereas the second configuration (S-BOCDR-2) [22] uses the light Fresnel-reflected at the proximal end of the FUT, which is a partial reflection point artificially produced near an optical circulator. One major drawback of S-BOCDR is that the measurement range is limited to one-half of the FUT length—the proximal half (distal to the open end) in S-BOCDR-1, and the distal half (proximal to the open end) in S-BOCDR-2. Although S-BOCDR-1 can be implemented more easily, S-BOCDR-2 is more advantageous from the perspective of end users because measurement of the distal half of the FUT length is more convenient for practical applications and because, even when the FUT has a breakage point, the measurement can be continued at least up to that point. However, two problems remain in implementing S-BOCDR-2; these are 1) the unstable power of the Stokes light that propagates through the partial reflection point (such as an air gap; extensive disturbance makes a distributed measurement difficult) and 2) the need for preparation of optical fibers with sufficiently different Brillouin frequency shift (BFS) values, which are inserted around the partial reflection point to suppress the influence of the 0th correlation peak.

In the meantime, distributed strain and temperature measurement based on Brillouin scattering in polymer optical fibers (POFs) has become an active area of research [23]–[28]. Owing to their unique features including high flexibility, POFs have potential applications in highly sensitive temperature sensing [24], cryogenic sensing [25], large-strain sensing [26], and sensing with a “memory” function [28]. Researchers have recently demonstrated (quasi-) distributed Brillouin sensing using POFs based on BOFDA [27] and BOCDR [28].

In this paper, we implement S-BOCDR-2 using a POF and show that the aforementioned two problems are mitigated. As for problem 1) mentioned above, the Stokes light can be stably returned from the POF through the interface between the POF and the silica single-mode fiber (SMF); this structure is simpler and more robust than that previously reported [22]. As for problem (2), the BFS in the POF can be irreversibly upshifted by  $\sim 300$  MHz only by applying large strain (named BFS hopping [29]). A distributed measurement is experimentally demonstrated, in which a 0.46-m-long heated POF section is successfully detected.

## 2. Principle

Brillouin scattering occurs as a result of an interaction between propagating light (or photons) and acoustic phonons in an optical fiber. This interaction generates Stokes light propagating in the direction opposite to that of the incident light. The central frequency of the Stokes light spectrum (termed as the Brillouin gain spectrum (BGS)) is lower than that of the incident light. The amount of this frequency shift is referred to as BFS, which is, at  $1.55 \mu\text{m}$ , typically  $\sim 10.8$  GHz for silica SMFs [1] and  $\sim 2.8$  GHz for perfluorinated graded-index (PFGI) POFs [23]. If a strain or temperature change is applied to the fiber, the BFS shifts towards a higher or lower frequency according to the fiber core material, which is the fundamental operating principle of fiber-optic Brillouin strain/temperature sensors. The strain- and temperature-dependence coefficients of the BFS in PFGI-POFs at  $1.55 \mu\text{m}$  have been reported to be  $-121.8$  MHz/% [24] (in the strain range below 1%) and  $-3.2$  MHz/K [25] (in the temperature range below  $85^\circ\text{C}$ ), which are  $-0.25$  and  $-3.2$  times those in silica SMFs [30], [31], respectively. This indicates that Brillouin scattering in PFGI-POFs has a great potential for highly sensitive temperature sensing with reduced strain sensitivity. Unique nonlinear BFS dependence at larger strain [24] and higher temperature [25] has been observed, which can be exploited to perform large-strain sensing and more sensitive temperature sensing, respectively. Another unique phenomenon is BFS hopping [29], in which the BFS in the PFGI-POF abruptly changes from  $\sim 2.8$  GHz to  $\sim 3.1$  GHz under a large strain of  $> 7.3\%$ .

In a standard BOCDR setup [10], [20], the beat signal of the Stokes light and the reference light is detected as a BGS. By sinusoidal modulation of the laser frequency, correlation peaks are periodically located along the FUT [32]; the distance between adjacent peaks is set to be longer than the FUT length so that only one correlation peak exists in the FUT. Correlation

peaks of any order can be located in the FUT by controlling the optical path-length difference between the pump and the reference paths. The correlation peak position can be scanned along the FUT by sweeping the frequency of the sinusoidal modulation; thus, a distributed BGS measurement can be performed.

In contrast, in S-BOCDR [21], [22], the laser output is injected directly into the FUT, and the reflected light (consisting not only of the Brillouin-Stokes light, but also of the reference light that is Fresnel reflected at one of the FUT ends) is detected. Two configurations of S-BOCDR have been developed so far; one (S-BOCDR-1) uses the light Fresnel-reflected at the open end of the FUT [21], while the other (S-BOCDR-2) uses the light Fresnel-reflected at the partial reflection point artificially induced near an optical circulator [22]. When the laser frequency is subject to sinusoidal modulation, correlation peaks are generated along the FUT. As the 0th correlation peak is fixed at a zero-optical-path-difference point, i.e., at the FUT open end (S-BOCDR-1) or at the partial reflection point (S-BOCDR-2), its influence needs to be suppressed, for example, by applying some artificial loss near the open end (S-BOCDR-1) or by replacing the nearby fibers with fibers that have different BFS values (S-BOCDR-2). The measurement range in both S-BOCDR schemes is limited to one-half of the FUT length: distal from the open end (S-BOCDR-1) or proximal from the open end (S-BOCDR-2), the latter of which is more convenient for practical applications. When the FUT has a breakage point, the measurement becomes non-feasible in S-BOCDR-1, although the measurement can be continued at least to that breakage point. Thus, broadly speaking, S-BOCDR-2 is superior in performance to S-BOCDR-1, from a practical viewpoint.

However, S-BOCDR-2 suffers from two problems. One is that the Stokes light is not stably returned from the FUT through the partial reflection point, leading to a low measurement stability. For instance, in our previous experiment [22], an air gap was used to induce partial reflection, which was susceptible to external disturbance. The other problem is that we need to prepare optical fibers with sufficiently different BFS values and insert them around the partial reflection point to suppress the influence of the 0th correlation peak. Silica multi-mode fibers with BFS values of  $\sim 10.5$  GHz were inserted in our previous experiment [22], though this necessity is undesirable.

Here, we show that these two problems of S-BOCDR-2 can be mitigated by implementing it using a POF as an FUT. Then, a partial reflection point can be automatically created at the butt-coupled interface between the POF and the silica SMF (the pigtail of an optical circulator) [23], at which Fresnel-reflected light with a reflectivity of 0.2% (calculated using  $n = 1.46$  in a silica SMF and 1.35 in a PFGI-POF) is obtained; the Stokes light can stably pass through the interface. The key to the solution of the second problem is the BFS hopping phenomenon [29], in which the BFS in the POF (BFS:  $\sim 2.8$  GHz) can be irreversibly upshifted by  $\sim 300$  MHz only by applying a large strain of  $> 7.3\%$ . Unless cryogenic sensing is the intended application, the BFS "upshift" is preferable because the BFS in a POF decreases with increasing applied strain [24] and temperature [24], [25]). Thus, instead of inserting different fibers around the butt-coupled part, we have only to pull the POF for a length sufficiently longer than half of the spatial resolution (i.e., the width of the 0th correlation peak). Note that, as the BGS of the silica SMF (BFS:  $\sim 10.8$  GHz) near the butt-coupled part does not overlap with that of the POF, it requires no modification.

### 3. Experimental Setup and Results

An S-BOCDR-2 setup using a POF as an FUT is schematically shown in Fig. 1. The pump light at  $1.55 \mu\text{m}$  was amplified up to  $\sim 30$  dBm using an erbium-doped fiber amplifier (EDFA) and was injected into the POF by an optical circulator. The optical beat signal of the Brillouin Stokes light and the Fresnel-reflected light was converted into an electrical signal using a photo detector (PD) and was observed using an electrical spectrum analyzer (ESA) as a BGS. All the optical paths except the FUT were composed of silica SMFs. The laser output frequency was sinusoidally modulated by direct modulation of the driving current [10], [19].

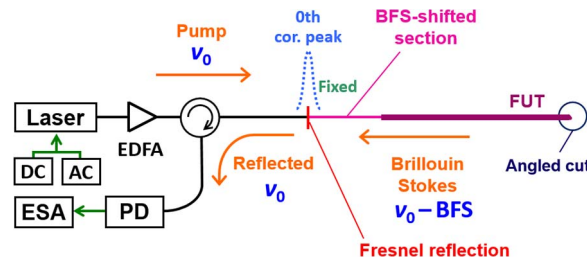


Fig. 1. Experimental setup of S-BOCDR-2 using a POF.

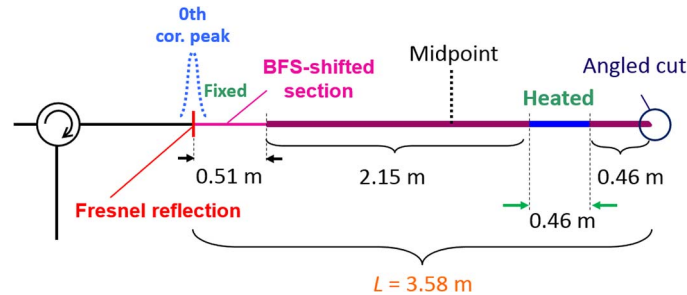


Fig. 2. Structure of the FUT.

As an FUT, we employed a 3.39-m-long PFGI-POF with 50  $\mu\text{m}$  core diameter, 70  $\mu\text{m}$  cladding diameter, and 490  $\mu\text{m}$  overcladding diameter. The core and cladding layers were composed of doped and undoped polyperfluorobutenylvinyl ether. The refractive index at the core center was 1.35, the numerical aperture was 0.185, and the propagation loss at 1.55  $\mu\text{m}$  was  $\sim 250$  dB/km. The detailed FUT structure is shown in Fig. 2. One end of the FUT was butt-coupled to a 1.05-m-long silica SMF (the pigtail of a circulator), and the other end was left open and cut with an angle to suppress the Fresnel reflection at that end. In order to suppress the influence of the 0th correlation peak generated at the butt-couple, a 0.32-m-long nearby section of the FUT was elongated and then released, resulting in a length of 0.51 m (corresponding to 59% strain). Consequently, the whole length of the FUT became 3.58 m, leading to a measurement range of 1.79 m. In this experiment, to clearly show the distributed measurability, we swept the modulation frequency  $f_m$  from 31.0366 MHz to 62.0732 MHz and fixed the modulation amplitude  $\Delta f$  at 1.33 GHz, corresponding to a spatial resolution of  $\sim 42$  mm at  $l = 0$  m (open end) and  $\sim 84$  mm at  $l = 1.79$  m (midpoint). These values were much smaller than twice the length of the BFS-shifted section. A 0.46-m-long section of the FUT near the open end was heated ( $< 70$   $^\circ\text{C}$ ), as shown in Fig. 2. The sampling rate at a single sensing point was 3.3 Hz (limited by the data acquisition from the ESA). There were 89 sensing points, and the measurement lasted for  $\sim 27$  s. The operating temperature was maintained at 24  $^\circ\text{C}$ .

First, the BGS over the whole length of the FUT was measured (see Fig. 3). The frequency of the laser output was fixed. The vertical axis was normalized so that the maximal power of the BGS was 1. The peak at  $\sim 2.79$  GHz corresponds to the BGS in the unstrained POF section [23], whereas the peak at  $\sim 3.11$  GHz corresponds to the BGS in the strained (BFS-shifted) POF section [29]. Thus, the BFS in the POF section around the butt-couple was verified to be upshifted.

Subsequently, the BGS distribution was measured when the FUT was locally ( $l = 0.46 - 0.92$  m) heated to 60  $^\circ\text{C}$ , as shown in Fig. 4(a), and the measured BGSs at  $l = 1.15$  m (room temperature) and at  $l = 0.59$  m (heated) are shown in Fig. 4(b). The vertical axes were normalized so that the maximal powers of all the BGSs were 1, because even the highest Stokes power of  $-84.68$  dBm was extremely close to the noise floor level of  $-84.78$  dBm. A BFS downshift was clearly observed at the heated section. The BFS distributions measured at different

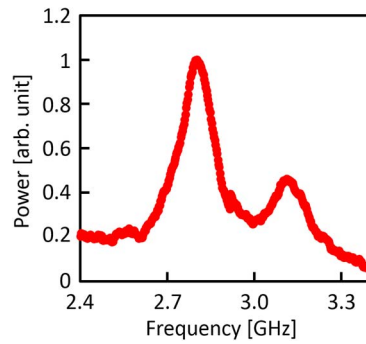


Fig. 3. Measured BGS in the whole length of the FUT.

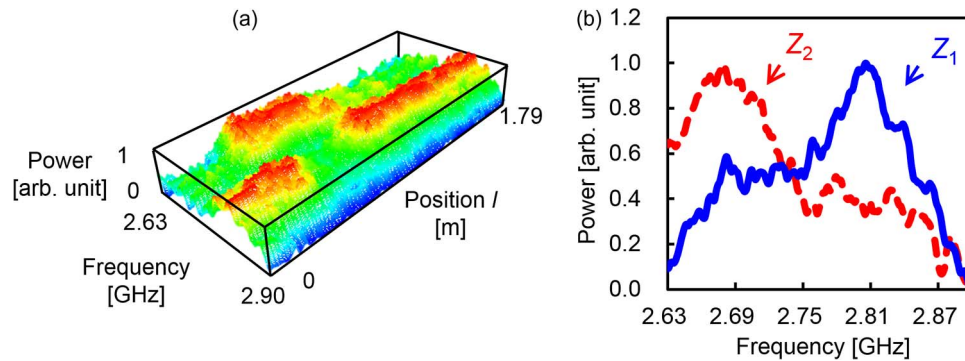


Fig. 4. (a) Measured BGS distribution when the FUT was locally heated to 60 °C. (b) Measured BGSs at  $l = 1.15$  m (room temperature;  $z_1$ ) and at  $l = 0.59$  m (heated;  $z_2$ ).

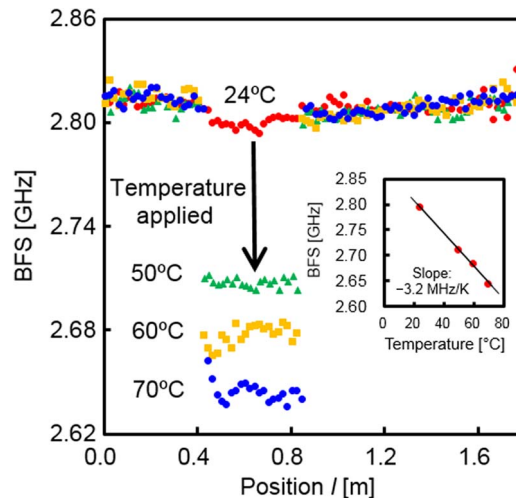


Fig. 5. Measured BFS distributions when the FUT was locally heated to 24, 50, 60, and 70 °C. The inset shows the measured BFS dependence on temperature change.

temperatures (24, 50, 60, and 70 °C) are shown in Fig. 5, where the 0.46-m-long heated section was successfully detected. As shown in the inset of Fig. 5, the BFS decreased with increasing temperature, with a proportionality constant of  $-3.2$  MHz/K (calculated using the BFS values at the midpoint of the heated section), which agrees well with a previously reported value [25]. The BFS fluctuations along the non-heated sections showed a standard deviation of approximately

$\pm 3.0$  MHz, corresponding to strain and temperature measurement errors of around  $\pm 0.02\%$  and  $\pm 0.9$  °C, respectively. Thus, a distributed measurement capability of S-BOCDR-2 using a POF was demonstrated.

#### 4. Conclusion

Two problems in the second configuration of S-BOCDR—instability of the Stokes light and necessity of a cumbersome method for suppressing the 0th correlation peak—were shown to be mitigated by employing a POF as an FUT. In POF-based S-BOCDR, the beat signal of the Stokes light and the Fresnel-reflected light generated at the POF/SMF interface can be stabilized, and the influence of the 0th correlation peak can be easily suppressed by using the BFS hopping phenomenon. In a pilot distributed measurement, a 0.46-m-long heated POF section was successfully detected. We anticipate that, owing to its extreme simplicity, POF-based S-BOCDR will be one of the promising techniques in implementing distributed strain/temperature Brillouin sensors in the near future.

---

#### References

- [1] G. P. Agrawal, *Nonlinear Fiber Optics* Academic. San Diego, CA, USA, 1995.
- [2] S. Norcia, S. Tonda-Goldstein, D. Dolfi, and J. P. Huignard, "Efficient single-mode Brillouin fiber laser for low-noise optical carrier reduction of microwave signals," *Opt. Lett.*, vol. 28, no. 20, pp. 1888–1890, Oct. 2003.
- [3] Z. Zhu, D. J. Gauthier, and R. W. Boyd, "Stored light in an optical fiber via stimulated Brillouin scattering," *Science*, vol. 318, no. 5857, pp. 1748–1750, Dec. 2007.
- [4] E. A. Kuzin, M. P. Petrov, and B. E. Davydenko, "Phase conjugation in an optical fibre," *Opt. Quantum Electron.*, vol. 17, no. 6, pp. 393–397, Nov. 1985.
- [5] K. Y. Song, M. G. Herraiez, and L. Thevenaz, "Observation of pulse delaying and advancement in optical fibers using stimulated Brillouin scattering," *Opt. Exp.*, vol. 13, no. 1, pp. 82–88, Jan. 2005.
- [6] T. Horiguchi and M. Tateda, "BOTDA-nondestructive measurement of single-mode optical fiber attenuation characteristics using Brillouin interaction: Theory," *J. Lightw. Technol.*, vol. 7, no. 8, pp. 1170–1176, Aug. 1989.
- [7] T. Kurashima, T. Horiguchi, H. Izumita, and M. Tateda, "Brillouin optical-fiber time domain reflectometry," *IEICE Trans. Commun.*, vol. E76-B, pp. 382–390, 1993.
- [8] D. Garus, K. Krebber, and F. Schliep, "Distributed sensing technique based on Brillouin optical-fiber frequency-domain analysis," *Opt. Lett.*, vol. 21, no. 8, pp. 1402–1404, Sep. 1996.
- [9] K. Hotate and T. Hasegawa, "Measurement of Brillouin gain spectrum distribution along an optical fiber using a correlation-based technique—Proposal, experiment and simulation," *IEICE Trans. Electron.*, vol. E83-C, no. 405–412, 2000.
- [10] Y. Mizuno, W. Zou, Z. He, and K. Hotate, "Proposal of Brillouin optical correlation-domain reflectometry (BOCDR)," *Opt. Exp.*, vol. 16, no. 16, pp. 12 148–12 153, Aug. 2008.
- [11] K. Y. Song and H. J. Yoon, "High-resolution Brillouin optical time domain analysis based on Brillouin dynamic grating," *Opt. Lett.*, vol. 35, no. 1, pp. 52–54, Jan. 2010.
- [12] Y. Peled, A. Motil, and M. Tur, "Fast Brillouin optical time domain analysis for dynamic sensing," *Opt. Exp.*, vol. 20, no. 8, pp. 8584–8591, Apr. 2012.
- [13] U. Javier, S. Mikel, and L. Alayn, "Phasorial differential pulse-width pair technique for long-range Brillouin optical time-domain analysis sensors," *Opt. Exp.*, vol. 22, no. 14, pp. 17 403–17 408, Jun. 2014.
- [14] R. Bernini, A. Minardo, and L. Zeni, "Distributed sensing at centimeter-scale spatial resolution by BOFDA: Measurements and signal processing," *IEEE Photon. J.*, vol. 4, no. 1, pp. 48–56, Feb. 2012.
- [15] A. Wosniok, Y. Mizuno, K. Krebber, and K. Nakamura, "L-BOFDA: A new sensor technique for distributed Brillouin sensing," in *Proc. 5th EWOFs*, Krakow, Poland, 2013, pp. 8794–8798.
- [16] K. Y. Song, Z. He, and K. Hotate, "Distributed strain measurement with millimeter-order spatial resolution based on Brillouin optical correlation domain analysis," *Opt. Lett.*, vol. 31, no. 17, pp. 2526–2528, Sep. 2006.
- [17] R. K. Yamashita, W. Zou, Z. He, and K. Hotate, "Measurement range elongation based on temporal gating in Brillouin optical correlation domain distributed simultaneous sensing of strain and temperature," *IEEE Photon. Technol. Lett.*, vol. 24, no. 12, pp. 1006–1008, Jun. 2012.
- [18] W. Zou, Z. He, and K. Hotate, "Range elongation of distributed discrimination of strain and temperature in Brillouin optical correlation-domain analysis based on dual frequency modulations," *IEEE Sens. J.*, vol. 14, no. 1, pp. 244–248, Jan. 2014.
- [19] Y. Mizuno, Z. He, and K. Hotate, "One-end-access high-speed distributed strain measurement with 13-mm spatial resolution based on Brillouin optical correlation-domain reflectometry," *IEEE Photon. Technol. Lett.*, vol. 21, no. 7, pp. 474–476, Apr. 2009.
- [20] Y. Mizuno, W. Zou, Z. He, and K. Hotate, "Operation of Brillouin optical correlation-domain reflectometry: Theoretical analysis and experimental validation," *J. Lightw. Technol.*, vol. 28, no. 22, pp. 3300–3306, Nov. 2010.
- [21] N. Hayashi, Y. Mizuno, and K. Nakamura, "Simplified configuration of Brillouin optical correlation-domain reflectometry," *IEEE Photon. J.*, vol. 6, no. 5, Oct. 2014, Art. ID. 6802807.

- [22] N. Hayashi, Y. Mizuno, and K. Nakamura, "Alternative implementation of simplified Brillouin optical correlation-domain reflectometry," *IEEE Photon. J.*, vol. 6, no. 6, Dec. 2014, Art. ID. 6803108.
- [23] Y. Mizuno and K. Nakamura, "Experimental study of Brillouin scattering in perfluorinated polymer optical fiber at telecommunication wavelength," *Appl. Phys. Lett.*, vol. 97, no. 8, 2010, Art. ID. 021103.
- [24] Y. Mizuno and K. Nakamura, "Potential of Brillouin scattering in polymer optical fiber for strain-insensitive high-accuracy temperature sensing," *Opt. Lett.*, vol. 35, no. 23, pp. 3985–3987, Dec. 2010.
- [25] K. Minakawa *et al.*, "Wide-range temperature dependences of Brillouin scattering properties in polymer optical fiber," *Jpn. J. Appl. Phys.*, vol. 53, no. 4, Apr. 2014, Art. ID. 042502.
- [26] N. Hayashi, Y. Mizuno, and K. Nakamura, "Brillouin gain spectrum dependence on large strain in perfluorinated graded-index polymer optical fiber," *Opt. Exp.*, vol. 20, no. 19, pp. 21 101–21 106, Sep. 2012.
- [27] A. Minardo, R. Bernini, and L. Zeni, "Distributed temperature sensing in polymer optical fiber by BOFDA," *IEEE Photon. Technol. Lett.*, vol. 26, no. 4, pp. 387–390, Feb. 2014.
- [28] N. Hayashi, Y. Mizuno, and K. Nakamura, "Distributed Brillouin sensing with centimeter-order spatial resolution in polymer optical fibers," *J. Lightw. Technol.*, vol. 32, no. 21, pp. 3397–3401, Nov. 2014.
- [29] N. Hayashi, K. Minakawa, Y. Mizuno, and K. Nakamura, "Brillouin frequency shift hopping in polymer optical fiber," *Appl. Phys. Lett.*, vol. 105, no. 9, Sep. 2014, Art. ID. 091113.
- [30] T. Horiguchi, T. Kurashima, and M. Tateda, "Tensile strain dependence of Brillouin frequency shift in silica optical fibers," *IEEE Photon. Technol. Lett.*, vol. 1, no. 5, pp. 107–108, May 1989.
- [31] T. Kurashima, T. Horiguchi, and M. Tateda, "Thermal effects on the Brillouin frequency shift in jacketed optical silica fibers," *Appl. Opt.*, vol. 29, no. 15, pp. 2219–2222, May 1990.
- [32] K. Hotate, "Application of synthesized coherence function to distributed optical sensing," *Meas. Sci. Technol.*, vol. 13, no. 11, pp. 1746–1755, Nov. 2002.